Expert Systems With Applications 180 (2021) 115141

Contents lists available at ScienceDirect

Expert Systems With Applications

journal homepage: www.elsevier.com/locate/eswa

Determination of COVID-19 pneumonia based on generalized convolutional neural network model from chest X-ray images

Adi Alhudhaif [a], Kemal Polat [b,*], Onur Karaman [c]

[a] Department of Computer Science, College of Computer Engineering and Sciences in Al-kharj, Prince Sattam Bin Abdulaziz University, P.O. Box 151, Al-Kharj 11942, Saudi Arabia
[b] Department of Electrical and Electronics Engineering, Bolu Abant Izzet Baysal University, Bolu, Turkey
[c] Akdeniz University, Vocational School of Health Services, Department of Medical Imaging Techniques, Antalya 07070, Turkey

ARTICLE INFO

Keywords:
Corona Virus (COVID-19)
Convolutional Neural Network (CNN)
Deep learning
Chest X-ray images

ABSTRACT

X-ray units have become one of the most advantageous candidates for triaging the new Coronavirus disease COVID-19 infected patients thanks to its relatively low radiation dose, ease of access, practical, reduced prices, and quick imaging process. This research intended to develop a reliable convolutional-neural-network (CNN) model for the classification of COVID-19 from chest X-ray views. Moreover, it is aimed to prevent bias issues due to the database. Transfer learning-based CNN model was developed by using a sum of 1,218 chest X-ray images (CXIs) consisting of 368 COVID-19 pneumonia and 850 other pneumonia cases by pre-trained architectures, including DenseNet-201, ResNet-18, and SqueezeNet. The chest X-ray images were acquired from publicly available databases, and each individual image was carefully selected to prevent any bias problem. A stratified 5-fold cross-validation approach was utilized with a ratio of 90% for training and 10% for the testing (unseen folds), in which 20% of training data was used as a validation set to prevent overfitting problems. The binary classification performances of the proposed CNN models were evaluated by the testing data. The activation mapping approach was implemented to improve the causality and visuality of the radiograph. The outcomes demonstrated that the proposed CNN model built on DenseNet-201 architecture outperformed amongst the others with the highest accuracy, precision, recall, and F1-scores of 94.96%, 89.74%, 94.59%, and 92.11%, respectively. The results indicated that the reliable diagnosis of COVID-19 pneumonia from CXIs based on the CNN model opens the door to accelerate triage, save critical time, and prioritize resources besides assisting the radiologists.

1. Introduction

The new Coronavirus disease (COVID-19), caused by the SARS-CoV-2 virus, has been caused people to have an acute respiratory infection (Graham, Dela Cruz, Cao, Pasnick, & Jamil, 2020; Li, Liu, Yu, Tang, & Tang, 2020). COVID-19 was proclaimed as a "pandemic" by the World Health Organization (WHO) on March 11, 2020 (Li et al., 2020; Xu et al., 2020).

Dry cough, headache, difficulty breathing, weakness, and lack of smell and taste can be defined as general indications of the disease. On the other hand, in some extreme cases, dyspnea and/or hypoxemia can occur a week after the appearance of the disease, accompanied by septic shock, acute respiratory distress syndrome (ARDS), and dysfunction of coagulation (Wang et al., 2020; Holshue et al., 2020; Huang et al., 2020). The symptoms of COVID-19 can be recorded from all age ranges. However, those over 30 are the most infected, and the symptoms of the disease are more severe in elders, although the prevalence of infection in children and young adults is lower (Dong et al., 2020). According to reports, one of the most substantial steps in the struggle against COVID-19 is the early detection of infected individuals, followed by the launching of treatment protocols in serious cases, as well as quarantine procedures to avoid the spreading of disease (Polat et al., 2021). These steps are principally accompanied by the diagnostic protocol of COVID-19 disease; clinical symptoms; epidemiological history, and assessment of the viral nucleic acid test or radiology images (Ai et al., 2020; Chen et al., 2020; Wang et al., 2020). Although the real-time reverse transcription-polymerase chain reaction (RT-PCR) technique is acknowledged as a prevalent tool for the detection of the infected

* Corresponding author at: Bolu Abant Izzet Baysal University, Faculty of Engineering, Department of Electrical and Electronics Engineering, Bolu, Turkey.
E-mail addresses: A.alhudhaif@psau.edu.sa (A. Alhudhaif), kpolat@ibu.edu.tr (K. Polat), onurkaraman@akdeniz.edu.tr (O. Karaman).

https://doi.org/10.1016/j.eswa.2021.115141
Received 25 March 2021; Received in revised form 28 April 2021; Accepted 28 April 2021
Available online 4 May 2021
0957-4174/© 2021 Elsevier Ltd. All rights reserved.

patient, there are many limitations, such as a deficiency of test kits for tens of thousands of suspicious patients especially in hyper-affected areas, accessibility in rural areas, and relatively low sensitivity (60%-70%), and poor specificity compared to CT chest scans (Polat et al.,2021). On the other hand, the time-consuming procedure of the RT-PCR test is required specialization and offers relatively poor accurate diagnosis rates in the early stages of the disease (Wang et al., 2020; Kanne, Little, Chung, Elicker, & Ketai, 2020). Radiological imaging techniques including chest x-ray and computed tomography (CT) are other important tools utilized for COVID-19 screening (Xie et al., 2020; Lee, Ng, & Khong, 2020). However, the chest X-ray images or CT scans must be analyzed by a radiologist to extract the radiological patterns associated with COVID-19 pneumonia. CT technique is more time consuming and causes more radiation dose than x-ray imaging, moreover, computed tomography may not be available in many underdeveloped regions, whereas the x-ray radiology unit is a readily available and low-cost system (Ebrahim et al., 2020; Zhang et al., 2020). Utilizing x-ray units for COVID-19 detection may help to accelerate both the triaging step and initiation of the treatment protocol. Furthermore, the accessibility of the portable x-ray units allows diagnosis in an isolation apartment, house, etc., so that the possibility of spreading of the disease can be reduced. However, it is more difficult to detect the hallmarks of the disease from CXIs visually since the radiological patterns of COVID-19 pneumonia and other pneumonias are close to each other, and often certain symptoms can include encroachment with other pulmonary infections (Wang et al., 2020). Thus, the engineering of artificial intelligence-based automated techniques has gained substantial significance to detect COVID-19 at the early stages of the disease (Dourado et al., 2020; Parah et al., 2020; Rebouças Filho et al., 2014; Rodrigues et al., 2018). Utilizing high-accuracy artificial intelligence models in healthcare systems can both enhance patient comfort and ease the load on radiologists by facilitating treatment protocols (Madurai Elavarasan & Pugazhendhi, 2020). In addition, it may be possible to minimize the associated costs by utilizing artificial intelligence-supported models in healthcare. Therefore, the development of a reliable smart appliance that can process CXIs and rapidly detect COVID-19 pneumonia is revolutionary for on-site applications (Kulkarni, Seneviratne, Baig, & Ahmed Khan, ,2020).

Over the past decades, numerous studies inspired by the need for quick diagnosis by medical imaging have focused on deep-learning algorithm-based models have been published (Minaee, Kafieh, Sonka, Yazdani, & Jamalipour Soufi, 2020; Zhang et al., 2020). The performance parameters of proposed artificial intelligence models to detect the patients infected by COVID-19 from CT scans have been shown to be very accurate (Wang, Kang, & Ma, 2020; Gozes et al., 2020; Shan et al., 2020). On the other hand, it is noteworthy to note that utilizing CXIs for COVID-19 pneumonia diagnosis will offer a way to assist the radiologists with enhanced screening, as it can rapidly and cost-effectively detect cases of COVID-19 pneumonia. Thus, the researchers have focused on developing models based on CXIs. However, due to the limited number of available CXIs for COVID-19 pneumonia, many of the studies have been using similar databases. Indeed, it can be said that some of the databases may be biased since they have been created by using COVID-19 radiological images obtained from the articles (Vaid, Kalantar, & Bhandari, 2020; Cohen, Morrison, & Dao, 2020; Wang et al., 2017). Moreover, it has been realized that most of the images contain lossy-images since some of the image features like brightness, contrast, sharpness has been changed by the authors. Therefore, this work it is aimed to prevent the biased problem caused by the database and to develop a more reliable CNN model for binary classification of COVID-19 pneumonia from other cases of pneumonia. Moreover, each individual CXIs were re-checked by three radiology experts with 8, 12, and 19 years of experience to confirm the pneumonia type.

There are some valuable works based on the CNN model for the detection of COVID-19 pneumonia in the literature. One of these research assessed Inception V3, Xception, and ResNeXt architectures for COVID −19 screening from CXIs. The Xception model was reported to have the highest results with 97.97% accuracy (Jain, Gupta, & Taneja, 2020). In another work, a deep convolutional neural network model with an accuracy of 97.20% was developed for binary classification of COVID-19 cases from chest X-rays (Ouchicha et al., 2020). Similarly, in the other work, not only the binary but also the multi-class classification of COVID-19 cases have successfully detected from CXIs by the proposed model with an accuracy of 98.08% and 87.02%, respectively (Ozturk et al., 2020). Bassi and Attux. (2020) fine-tuned a two-step transfer learning approach to CNN architectures by using the images acquired from the ChestX-Ray14 database and achieved 99.4% test accuracy (Bassi and Attux,2020). Another automated tool for detection of COVID-19 based on CXIs was proposed by Ohata et al. (2020). In this work, various CNN architectures were retained to optimize to serve as feature extractors for CXIs. According to the performance results, the MobileNet architecture with support vector machine (SVM) classifier using a linear kernel suggested the best accuracy value of 98.5%. das Chagas et al. (2021) proposed a real-time Internet of Things (IoT) system to detect pneumonia from CXIs. The dataset consisted of 6,000 chest X-ray images of children. Twelve different CNN architectures were adapted to function as resource extractors. The results showed that the VGG19 architecture with the SVM classifier using the radial basis function kernel was the best model to detect pneumonia from the chest radiographs. The suggested model achieved 96.47%, 96.46%, and 96.46% for accuracy, F1 score, and precision values, respectively (das Chagas et al., 2021). In another work conducted by Singh et al. (2021) a pipeline was developed that utilized CXIs to detect COVID-19 pneumonia. The features extracted from CXIs were distinguished by Hybrid Social Group Optimization algorithm, following by they were used to classify CXIs using various classifiers. The SVM classifier offered the best performance with an accuracy of 99.65%. For early diagnosis of COVID-19 infection, Nayak, Nayak, Sinha, Arora and Pachori (2021) suggest a deep learning supported automated approach based on X-ray images. They examined the efficacy of eight pre-trained Convolutional Neural Network (CNN) models for COVID-19 classification, such as AlexNet, VGG-16, GoogleNet, MobileNet-V2, SqueezeNet, ResNet-34, ResNet-50, and Inception-V3. The models have been validated on publicly available chest X-ray images and the best performance was obtained by ResNet-34 with an accuracy of 98.33%.

Herein, a more reliable deep CNN model based on a transfer learning approach was developed to identify the patients infected by COVID-19 pneumonia by utilizing CXIs. The main idea of this work to generalize the model by minimizing the possible bias problem and enhance the reliability of the model by eliminating the possible biased CXIs by the radiology experts. Three different pre-trained architectures, including DenseNet-201, ResNet-18, and SqueezeNet, were used to trained the model and assessed by the calculated confusion matrices. The results indicated that the proposed CNN model could be utilized for binary classification of COVID-19 patients with high-performance parameters. The proposed model was trained, validated, and tested by real-world retrospective CXIs by clinically diagnosed with both COVID-19 pneumonia and other pneumonia. It can be speculated that the development of a reliable automated COVID-19 detection can reduce the workload of the clinician and helps to provide them with a second opinion.

2. Methods

2.1. Description of dataset

Herein, a total of 1,218 CXIs containing both COVID-19 pneumonia cases and other pneumonia cases were acquired from three publicly available databases including Kaggle (Kaggle, 2020), Cohen (Cohen et al., 2020), and Wang (Wang and Wong, 2020). The total number of COVID-19 pneumonia cases was reported as to be 3616, 208, 53 for Kaggle, Cohen, and Wang, respectively, whereas the number of other pneumonia cases was 1345, 41, 5526, respectively. To avoid the possible

bias problems caused by the database, each individual Chest X-ray image was systematically reviewed and selected by three thoracic radiologists with 8, 12, and 19 years of experience to make certain the type of pneumonia. These radiographs were reviewed independently and the final decision was reached by consensus. The readers were blinded from the clinical findings and the radiological reports of the patients. The CXIs were assessed for the presence, predominant pattern, and the distribution of lung parenchymal abnormalities. Subsequently, they were analyzed and categorized as either COVID-19 pnemonia or other pneumonia. The dominant pattern of lung parenchymal abnormality was assessed, the extent of involvement was recorded as unifocal, unilateral multifocal, or bilateral multifocal, and their distribution was then categorized as predominant central, peripheral or mixed. An opacity was considered central if most of the abnormality was located within the medial two-thirds of the lung, and was considered peripheral if most of it was located within the lateral one-third of the lung. The patterns of the lung parenchymal abnormalities were categorised as: consolidation; ground-glass; nodular opacities; or reticular opacities.

The reviewed CXIs acquired from different databases were combined with utilizing as the input of the developed CNN model. The average age of the selected X-ray images was found to be *ca.*57±3. The representative CXIs of COVID-19 pneumonias were illustrated in Fig. 1. Among these chest radiographs, 368 of them were labeled with COVID-19 pneumonia, whereas 850 of them were tagged with other pneumonia cases. The number of selected CXIs diagnosed with COVID-19 pneumonia cases was 300, 40, 28 from Kaggle, Cohen, and Wang databases, respectively, whereas the number of other pneumonia cases was 395, 19, 436 from Kaggle, Cohen, and Wang databases, respectively. A stratified 5-fold cross-validation approach was utilized with a ratio of 90% for training and %10 for the testing (unseen folds), in which 20% of training data was used as a validation set to prevent overfitting problems. 265 training, 66 validation, and 37 testing data were selected from COVID-19 Pneumonia cases, while these values were determined as 612 training, 153 validation, and 85 testing data for other pneumonia cases (Table 1).

2.2. Pre-processing of the images

All of the CXIs were normalized according to the pre-trained CNN architectures' standards. They were resized to 224 × 224 pixels to be ready for input to the various architectures, including SqueezeNet, DenseNet-201, ResNet-18. The number of COVID-19 pneumonia cases was almost two times smaller than the number of other pneumonia cases. Hence, in order to prevent the unbalanced data problem, as suggested in our previous work (Polat et al.,2021), an image augmentation approach was applied to each class to obtain additional training images. The description of the total number of CXIs was listed in Table 1. It is worth noting that while the COVID-19 pneumonia images were augmented six times, the images of other pneumonia cases were augmented only three times.

2.3. Transfer learning, optimization, and performance evaluation of the CNN model

Herein, binary-class classification of COVID-19 pneumonia from other pneumonia cases was carried out by utilizing the deep CNN models trained by the transfer learning approach (Fig. 2). Fastai, (2021) and OpenCV,(2021) frameworks were used to develop the model. Three deep networks including Residual Neural Network (ResNet) (He, Zhang, Ren, & Sun, 2016), Dense Convolutional Network (DenseNet) (Huang et al., 2017), and SqueezeNet (Simonyan and Zisserman, 2014) architectures, which have already been pre-trained by ImageNet (2021) database, were re-trained by transfer learning approach to develop the CNN model.

The stochastic gradient descent (SGD) approach was implemented to re-trained the selected CNN architectures (a detailed description can be found in our previous work Polat et al.,2021). The learning rate was determined as 10^{-2}, whereas the batch size and total backpropagation epochs were set to 16 images, 80 epochs, respectively. The confusion matrices were calculated by using the 5-fold cross-validation results to assess the performance of the DenseNet-201, ResNet-18, and SqueezeNet architectures.

2.4. Gradient-weighted class activation mapping

Gradient-weighted Class Activation Mapping (Grad-CAM) approach was implemented as reported in our previous work (Polat et al.,2021) to enhance the visuality by focusing attention on the critical regions of the CXIs. The regions where the model was activated were colored from the lowest activation to the highest activation from blue to red.

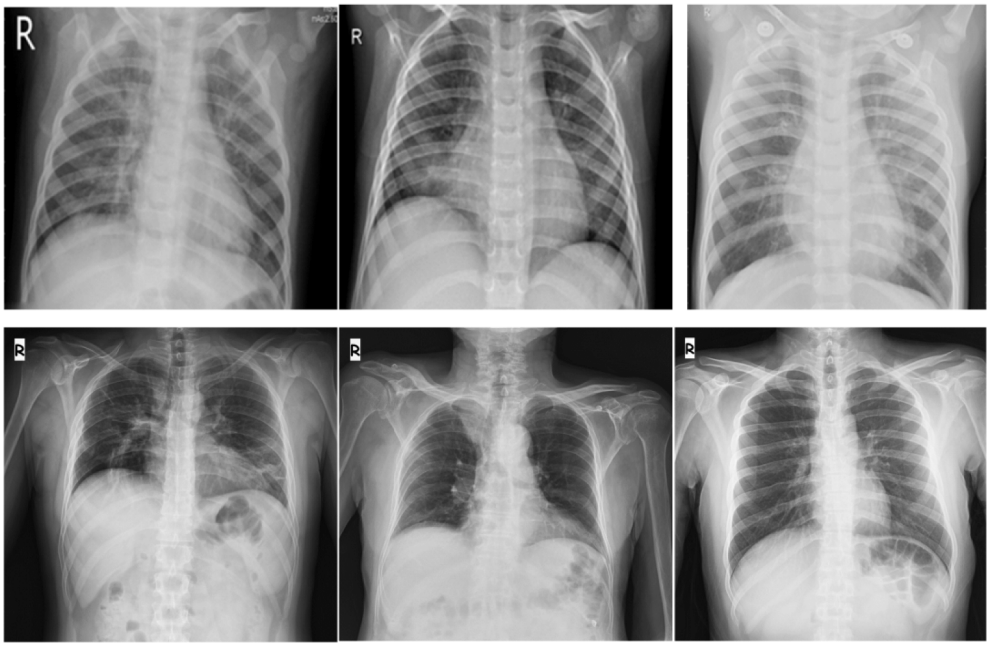

Fig. 1. Representative chest X-ray images for other pneumonia class (upper row) and COVID-19 pneumonia class (bottom row).

Table 1
Description of the total number of CXIs per class and per fold.

Class	Total Number of CXIs/Class	Training Set/Fold	Augmented Image/Fold	Validation Set/Fold	Testing
COVID-19 pneumonia	*368*	265	1,855	66	37
Other Pneumonia	*850*	612	1,836	153	85

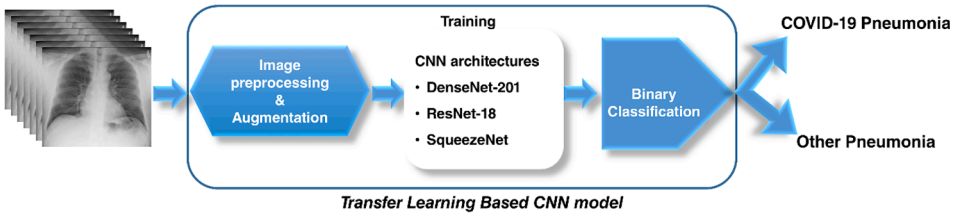

Fig. 2. The schematic illustration of the developed CNN model.

3. Results

Herein, the proposed CNN model was trained to detect and classify COVID-19 pneumonia and other pneumonia classes using CXIs (Scheme 1.). The 5-fold cross-validation approach was performed to assess the binary classification performance of the CNN model (Fig. 3.).

The proposed CNN model trained for a total of 80 epochs. At the end of each epoch, the validation loss, validation accuracy, and recall metrics of all architectures were calculated, and the findings were depicted in Fig. 4. The remarkable decrease in the validation loss values was detected at the beginning stage of the training process. Afterward, by reaching saturation, the curves were almost in steady-state conditions. The performance metrics of DenseNet-201 were calculated to be higher than the others.

The binary-class classification performance of the proposed CNN model was assessed by calculating the relevant confusion matrices for each fold. Then, the average performance matrix of each CNN architecture was obtained. The results indicated that their performance patterns were not far from each other. However, amongst them, it was observed that DenseNet-201 performed better than the others. The confusion matrices in all folds beside the overlapped-confusion matrices were presented in Fig. 5. The mean accuracy values to classify COVID-19 pneumonias and other pneumonias were calculated as 95.62%, 93.15%, and 92.97% for DenseNet-201, ResNet-18, and SqueezeNet architectures, respectively.

The performance metrics of each architecture for each fold were tabulated in Table 2. It was apparent that all the models were satisfactory in the binary classification of COVID-19 pneumonia and the other pneumonia classes. On the other hand, it should be noted that DenseNet-201 architecture, a relatively deeper network, offered the best performance in accuracy, recall, precision, and F1-score metrics.

The confusion matrices were also calculated for testing data (Fig. 6). The related performance metrics of each architecture for testing data were presented in Table 3. As can be seen from Table 3, it has been proven that DenseNet-201 architecture outperforms other architectures. DenseNet-201′s confusion matrix (Fig. 5A) revealed that the developed model was able to detect 35 out of 37 patients with COVID-19 pneumonia with COVID-19, 79 out of 82 non-COVID pneumonia cases like other pneumonia. Additionally, it was seen that 5.41% misclassified COVID-19 pneumonia cases. The developed CNN model based on DenseNet-201 architecture offered the best performance metrics of 94.96%, 89.74%, 94.59%, and 92.11% as accuracy, precision, recall, and F1-score, respectively. The satisfactory precision and the F1-score values showed that the proposed model performed confiding in classifying most of the CXIs. Morever, it was observed that CNN model based on DenseNet-201 architecture reached a test time of 0.470 ms. It can be speculated that it would be beneficial for practical applications.

Furthermore, the activation mapping of CXIs was performed by the

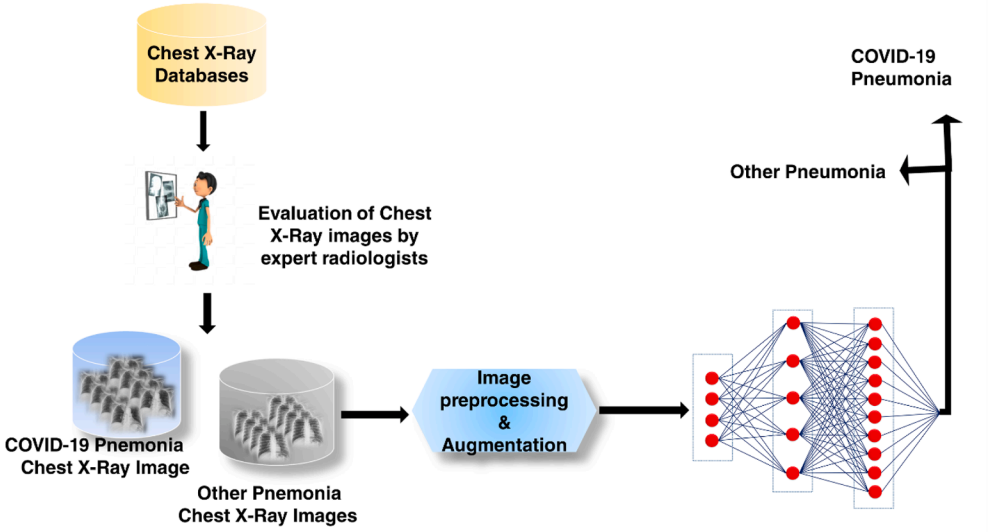

Scheme 1. Representative flowchart of proposed CNN approach.

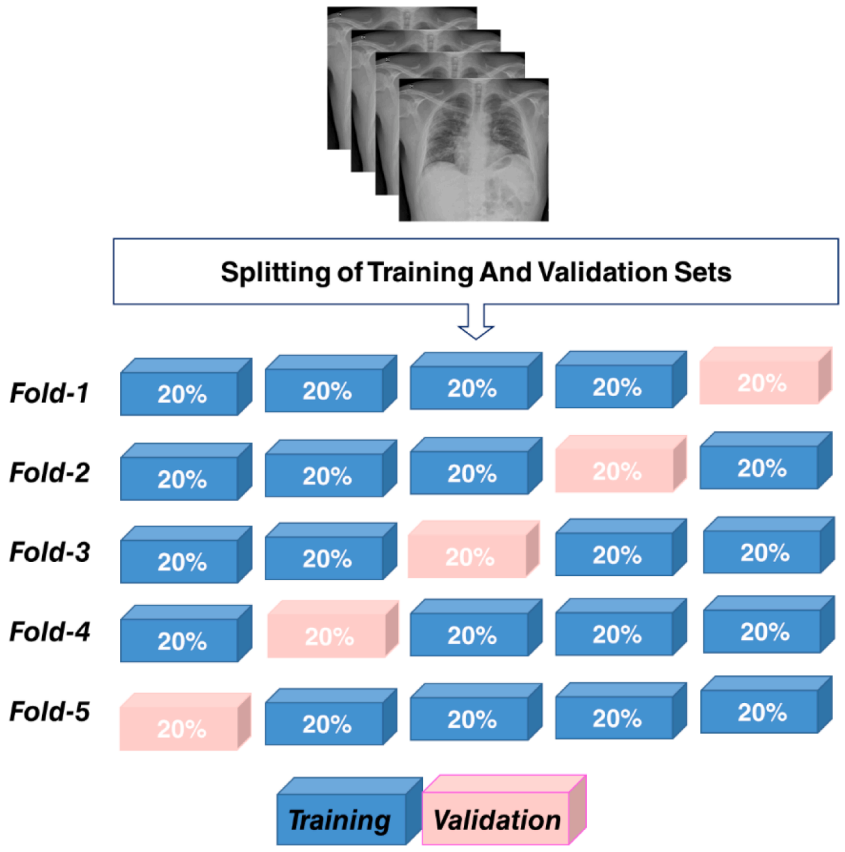

Fig. 3. Schematic illustration of 5-fold cross-validation approach.

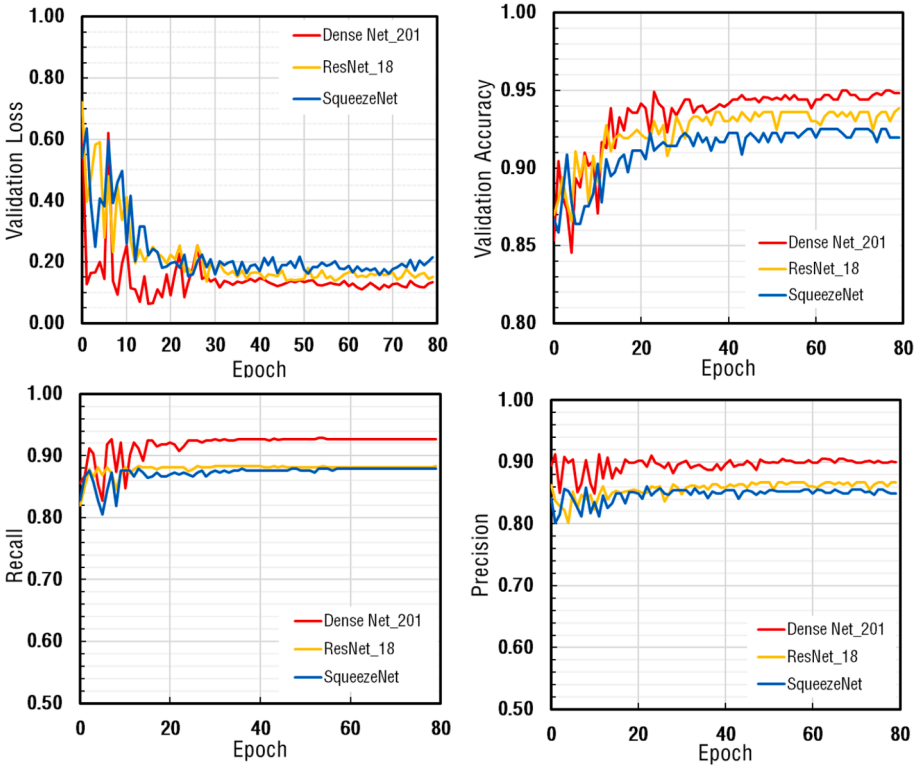

Fig. 4. The comparison of performance metrics for DenseNet-201, ResNet-18, SqueezeNet architectures obtained in Fold-1 for the CNN model.

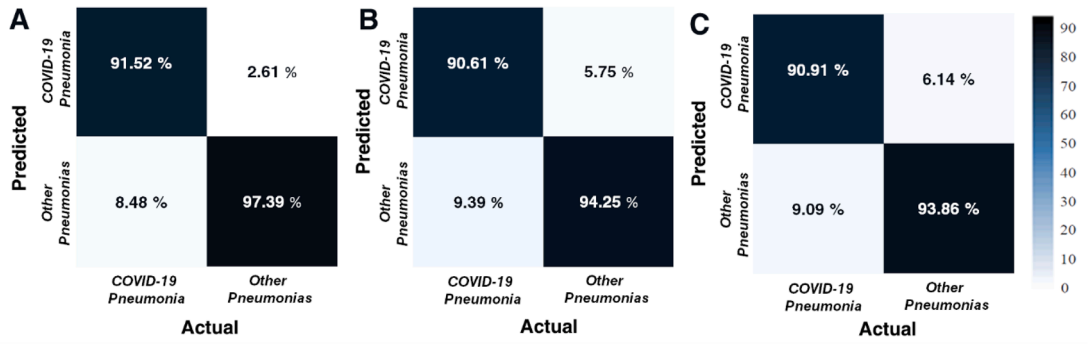

Fig. 5. The overlapped confusion matrices of validation data for (A) DenseNet-201, (B) ResNet-18, and (C) SqueezeNet architectures.

Table 2
The calculated performance metrics of the proposed model.

	DenseNet_201							
	TP	FP	FN	TN	Accuracy(%)	Precision (%)	Recall(%)	F1-score
Fold-1	61	7	5	146	94.52	89.71	92.42	91.04
Fold-2	58	3	8	150	94.98	95.08	87.88	91.34
Fold-3	60	2	6	151	96.35	96.77	90.91	93.75
Fold-4	61	5	5	148	95.43	92.42	92.42	92.42
Fold-5	62	3	4	150	96.80	95.38	93.94	94.66
Total	302	20	28	745	95.62	93.79	91.52	92.64
	ResNet_18							
	TP	**FP**	**FN**	**TN**	**Accuracy(%)**	**Precision(%)**	**Recall(%)**	**F1-score**
Fold-1	58	9	8	144	92.24	86.57	87.88	87.22
Fold-2	59	13	7	140	90.87	81.94	89.39	85.51
Fold-3	61	8	5	145	94.06	88.41	92.42	90.37
Fold-4	61	11	5	142	92.69	84.72	92.42	88.41
Fold-5	60	3	6	150	95.89	95.24	90.91	93.02
Total	299	44	31	721	93.15	87.17	90.61	88.86
	SqueezeNet							
	TP	**FP**	**FN**	**TN**	**Accuracy(%)**	**Precision(%)**	**Recall(%)**	**F1-score**
Fold-1	58	11	8	142	91.32	84.06	87.88	85.93
Fold-2	60	9	6	144	93.15	86.96	90.91	88.89
Fold-3	59	10	7	143	92.24	85.51	89.39	87.41
Fold-4	61	12	5	141	92.24	83.56	92.42	87.77
Fold-5	62	5	4	148	95.89	92.54	93.94	93.23
Total	300	47	30	718	92.97	86.46	90.91	88.63

TP: True Positive; FP:False Positive; FN: False Negative; TN: False Positive.

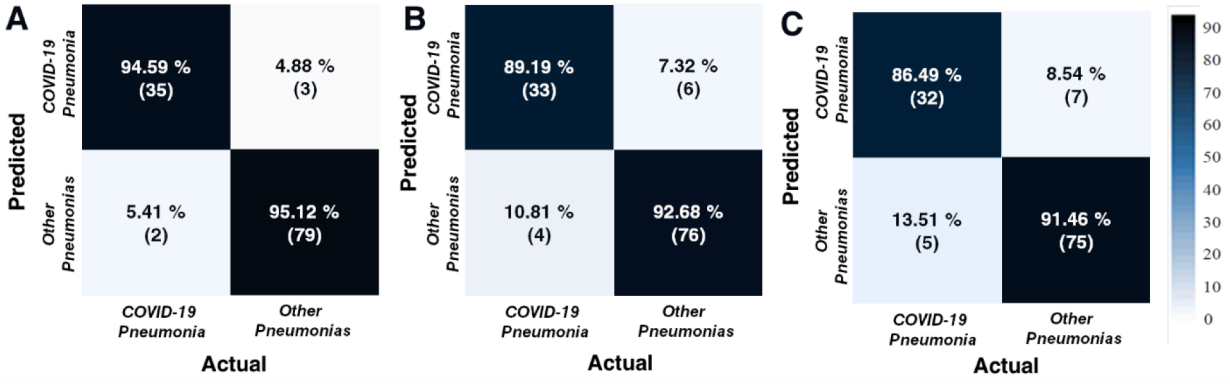

Fig. 6. The calculated confusion matrices of testing data for (A) DenseNet-201, (B) ResNet-18, and (C) SqueezeNet architectures.

Grad-CAM algorithm to enhance the visuality by emphasizing the crucial areas of the infected lung (Fig. 7.). The output of the activation mapping can offer an alternative opinion to the physician to detect COVID-19 pneumonia. As depicted in Fig. 7, it can be emphasized that the different colored regions represented the main areas that played a crucial role in CNN's decision-making process. As a result, it was concluded that the proposed model could be beneficial to reducing time to the decision-making process by assisting the radiologists. As can be seen from Fig. 7, while COVID-19 pneumonia case was detected bilateral and predominantly located in the central region, other pneumonia cases were locally seen in the lower parts of the lung.

4. Discussion

The early and rapid diagnosis, as well as faster triaging, are the key factors in controlling and preventing the spreading of COVID-19. Hence,

Table 3
The performance metrics of each architecture for testing data.

Architecture	Test Time(ms)	Performance Metrics Accuracy	Precision	Recall	F1-score
DenseNet_201	**0.470**±0.024	**94.96**	**89.74**	**94.59**	**92.11**
ResNet_18	0.583±0.008	91.60	84.62	89.19	86.84
SqueezeNet	0.771±0.115	89.92	82.05	86.49	84.21

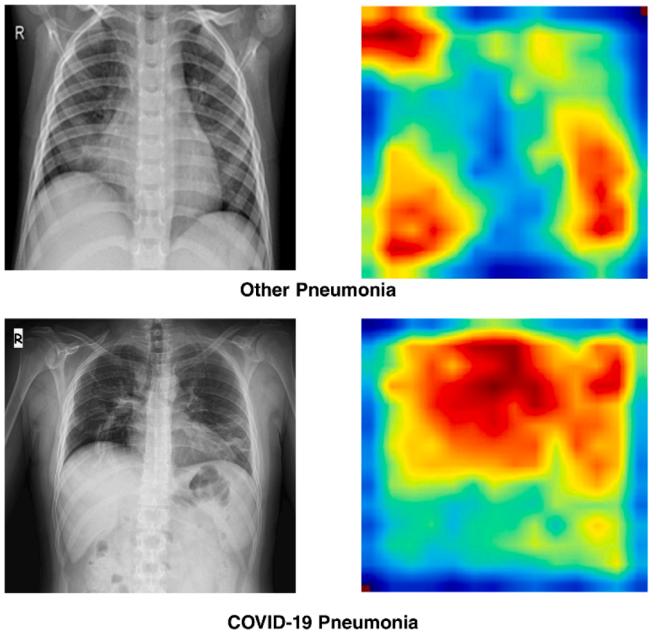

Fig. 7. The representative illustration of original chest X-ray images (left-side) and Grad-CAM activation mapping (right-side) of other pneumonia and COVID-19 pneumonia cases.

the development of time-efficient diagnostic tools seems to be crucial for the early detection of disease, treatment, and the isolation stages of the pandemic. Amongst the traditional techniques, the artificial intelligence-based smart models have gain prominence since they offer some advantageous characteristics such as high accuracy, rapid and easy-apply. Benefiting from the CXIs to classify COVID-19 pneumonia brings some crucial advantages such as having a lower radiation dose than computer tomography, being practical and accessible, and cost-neutral. Furthermore, CXIs are of a low-cost comparing to CT scans and easy access. However, it is relatively hard to detect COVID-19 from CXIs rather than chest CT images since CXIs have only a few characteristic features ascribed to COVID-19 pneumonia. Thus, it has great importance to utilize an artificial intelligence-based model for classifying COVID-19 from chest X-ray views. Machine learning models are sensitive to classify COVID-19 pneumonia by detecting the pathognomonic findings, including consolidation areas and nodular opacities. The proposed deep learning-based models are important to provide early and fast treatment besides avoiding the spreading of illness. As tabulated in Table 4. there are several high-quality pieces of research developed artificial intelligence models with high accuracy values to detect COVID-19 pneumonia by using CXIs. However, the main subject that should be noted is most of them used similar publicly available databases to train the model, causing the bias problem since there is a limited number of data for COVID-19 cases. In some datasets, the chest radiographs have been created by COVID-19 radiological images obtained from the articles. They even consist of lossy-images since their image properties, such as brightness, contrast, sharpness, etc., have already been adjusted by the authors (Che Azemin et al., 2020). Thus, it can be speculated that the works based on these databases may be

Table 4
The comparison of related studies for the automatic analysis of COVID-19 pneumonia from chest x-ray imaging utilizing artificial intelligence.

Study	Number of Cases	Data Source COVID-19	Accuracy (%)
Wang and Wong (2020)	53 COVID-19 (+)5526 COVID-19 (-)8066 Healthy	Wang	93.30
Polat et al. (2021)	299 COVID-191522 Pneumonia	Cohen	97.10
Sethy, Behera, Ratha, and Biswas (2020)	25 COVID-19 (+)25 COVID-19 (-)	Cohen	95.38
Luz, Silva, Silva, and Moreira (2020)	183 COVID-19 (+)8066 Healthy	Wang	94.30
Khobahi et al. (2020)	76 COVID-19 (+)5526 Pneumonia8066 Healthy	Cohen	93.50
Zhang, Xie, Li, Shen, and Xia (2020)	493 COVID-19 (+)24,596 Pneumonia18,774 Healthy	Cohen, Kaggle	83.61
Rahimzadeh and Attar (2020)	118 COVID-19 (+)6037 Pneumonia8868 Healthy	Cohen	91.40
Hall, Paul, Goldgof, and Goldgof (2020)	135 COVID-19 (+)208 Pneumonia	Cohen, SIRM, Radiopeadia	93.12
Majeed, Rashid, Ali, and Asaad, (2020)	184 COVID-19 (+)6290 Healthy	Cohen, Kaggle	97.00
El Asnaoui and Chawki (2020)	231 COVID-19 (+)4273 Pneumonia1583 Healthy	Cohen	92.18
This study	**368 COVID-19 (+)850 Other Pneumonia**	**Combined dataset(Kaggle, Cohen, Wang)**	**94.96**

biased, so they have reached unreliable superb accuracy values. Most of the reported CNN models provide high classification performance in a range of 93–99%. Moreover, it is noticed that some of the work used different radiological images belonging to different age groups such as childhood and elderly. It can be predicted that it also causes a bias problem.

Bearing all in mind, herein deep CNN models based on different pre-trained architectures have been developed to detect COVID-19 pneumonia from chest radiographs. In this work, a total of 1218 the CXIs (368 COVID-19 pneumonias, 850 other pneumonia) acquired from different publically available databases have been used to train the CNN model. To eliminate the probable bias problem, each individual CXIs was re-checked by three radiology experts to confirm the pneumonia type. Additionally, the average age of the selected CXIs was found to be *ca.*57±3. Also, superior care was taken not to select CXIs consisting of lossy-images, causing bias problems. As a result of image selection, a total of 368 CXIs labeled with COVID-19 pneumonia have been used, whereas some studies prior to this study have used 125, 25, 50 images in each class (Hemdan, Shouman, & Karar, 2020; Ozturk et al., 2020; Wang et al., 2020; Narin et al., 2020; Sethy, Behera, Ratha, & Biswas, 2020).

In this work, the CNN model built on DenseNet-201 pre-trained architecture has reached the highest accuracy value of 94.96% for binary classification of COVID-19 pneumonia and other pneumonia classes. More reliable performance metrics have been obtained compared to the other studies in the literature since the proposed model does not contain biased data. In this work, although a similar training approach suggested in our previous work has been followed, it is observed that the proposed CNN models offer lower accuracy values. The main reason for this can be attributed to the biased CXIs acquired directly from the publically available database despite the development of a de-biasing data loader in the previous study. In our previous work, to overcome the probable aforementioned bias problem, the CXIs without JPEG artifacts were recorded in JPEG format by changing the IMWRITE_JPEG_QUALITY value between 30 and 70 randomly with the *imwrite()* method in the OpenCV library. Furthermore, the bias problem was tried to be solved by

adding random brightness, contrast, sharpness adjustments in addition to JPEG artifacts to this data (Polat et al., 2021).

The main outcomes and contributions of this work can be listed as follows:

- The model has been generalized by eliminating the bias problem via using selected CXIs.
- Deeper pre-trained architectures such as DenseNet-201 have been outperformed to extract COVID-19 pneumonia from other pneumonia cases with significant specificity.
- The proposed model based on DenseNet-201 architecture has the highest accuracy value as 94.96%.
- The radiologist can also have been assisted by creating the activation maps of the original radiographs since they boost the causality and visuality.
- The proposed model is more a reliable and effective approach to assist the radiologists besides reducing the workload of experts.
- The patients diagnosed with COVID-19 pneumonia via the proposed CNN model can directly be transferred to the advanced centers, followed by treatment. Thus, it spreading of the disease can be avoided.
- The model has the ability to assess whether a patient infected with COVID-19 pneumonia or not within seconds.

5. Conclusion

Herein, the transfer learning approach has been used to developed a CNN model for screening of COVID-19 pneumonia from CXIs. The results reported in similar studies are biased and the reliability is controversial since most of the images in the database contain the lossy-images caused by the feature adjustment of the authors. Therefore, considering this problem, it is aimed to develop a generalized CNN model to prevent bias problems caused by the databases. The results have proved that the proposed CNN model based on DenseNet-201 can be utilized for automated detection of COVID-19 cases from CXIs. The binary classification accuracy, precision, recall, and F1-score values of the best CNN model built on DenseNet-201 have been obtained as 94.96%, 89.74%, 94.59%, and 92.11% respectively. In a nutshell, it can be concluded the proposed CNN model for screening COVID-19 based on CXIs is of great importance for the healthcare system thanks to the reduced diagnosis time, lowered radiation dose, as well as its lower cost. In this way, it is a crucial step for both accelerating diagnosis/treatment and controlling the spreading risk of the COVID-19 virus.

Ethical Approval

This study does not require an ethics committee.

Author statements

All the authors actively participated in the literature analysis, the interpretation of results and the preparation of the manuscript. All authors read and approved the final manuscript.

On the behalf of the all authors.

Declaration of Competing Interest

The authors declare that they have no known competing financial interests or personal relationships that could have appeared to influence the work reported in this paper.

Acknowledgements

This publication was supported by the Deanship of Scientific Research at Prince Sattam bin Abdulaziz University, Alkharj, Saudi Arabia.

References

Ai, T., Yang, Z., Hou, H., Zhan, C., Chen, C., Lv, W., et al. (2020). Correlation of chest CT and RT-PCR testing in coronavirus disease 2019 (COVID-19) in China: A report of 1014 cases. *Radiology, 296*, Article 200642. https://doi.org/10.1148/radiol.2020200642

Bassi, P.R., Attux, R., (2020). A deep convolutional neural network for COVID-19 detection using chest X-rays. arXiv preprint:2005.01578.

Che Azemin, M. Z., Hassan, R., Mohd Tamrin, M. I., & Md Ali, M. A. (2020). COVID-19 deep learning prediction model using publicly available radiologist-adjudicated chest X-ray images as training data: Preliminary findings. *Journal of Biomedical Imaging & Bioengineering, 2020*, 1–7. https://doi.org/10.1155/2020/8828855

Chen, N., Zhou, M., Dong, X., Qu, J., Gong, F., Han, Y., et al. (2020). Epidemiological and clinical characteristics of 99 cases of 2019 novel coronavirus pneumonia in Wuhan, China: A descriptive study. *Lancet, 395*(10223), 507–513. https://doi.org/10.1016/S0140-6736(20)30211-7

Cohen, J.P., Morrison, P., & Dao, L. (2020). COVID-19 image data collection, https://github.com/ieee8023/covid-chestxray-dataset.

das Chagas, J. V. S., Rodrigues, D. D. A., Ivo, R. F., Hassan, M. M., de Albuquerque, V. H. C., & Rebouças Filho, P. P. (2021). A new approach for the detection of pneumonia in children using CXR images based on an real-time IoT system. *Journal of Real-Time Image Processing*, 1–16. https://doi.org/10.1007/s11554-021-01086-y

Dong, Y., Mo, X.i., Hu, Y., Qi, X., Jiang, F., Jiang, Z., et al. (2020). Epidemiology of COVID-19 among children in China. *Pediatrics, 145*(6), e20200702. https://doi.org/10.1542/peds.2020-0702

Dourado, C. M. J. M., da Silva, S. P. P., da Nobrega, R. V. M., Reboucas Filho, P. P., Muhammad, K., & de Albuquerque, V. H. C. (2020). An open IoHT-based deep learning framework for online medical image recognition. *IEEE Journal on Selected Areas in Communications, 39*(2), 541–548. https://doi.org/10.1109/JSAC.4910.1109/JSAC.2020.3020598

Ebrahim, S. H., Ahmed, Q. A., Gozzer, E., Schlagenhauf, P., Memish, Z. A., et al. (2020). Covid-19 and community mitigation strategies in a pandemic. *British Medical Journal, 368*, Article m1066. https://doi.org/10.1136/bmj.m1066

El Asnaoui, K., & Chawki, Y. (2020). Using X-ray images and deep learning for automated detection of coronavirus disease. *Journal of Biomolecular Structure and Dynamics, 1–12*. https://doi.org/10.1080/07391102.2020.1767212

Madurai Elavarasan, R., & Pugazhendhi, R. (2020). Restructured society and environment: A review on potential technological strategies to control the COVID-19 pandemic. *Science of the Total Environment, 725*, 138858. https://doi.org/10.1016/j.scitotenv.2020.138858

Fastai (2021) Making neural nets uncool again, Fast.ai. https://www.fast.ai/ (Accessed March 15 2021).

Gozes, O., Frid-Adar, M., Greenspan, H., Browning, P. D., Zhang, H., Ji, W., Bernheim, A., & Siegel, E. (2020). Rapid AI development cycle for the coronavirus (COVID-19) pandemic: Initial results for automated detection & patient monitoring using deep learning CT image analysis. arXiv, preprint:2003.05037.

Graham, C. W., Dela Cruz, Cao, B., Pasnick, S., & Jamil, S. (2020). Novel Wuhan (2019-NCoV) coronavirus. *American Journal of Respiratory and Critical Care Medicine, 201*(4), 7–8. https://doi.org/10.1164/rccm.2014P7

Hall, L. O., Paul, R., Goldgof, D. B., & Goldgof, G. M. (2020). Finding covid-19 from chest x-rays using deep learning on a small dataset. arXiv preprint:2004.02060.

He, K., Zhang, X., Ren, S., & Sun, J. (2016). Deep residual learning for image recognition, In: Proceedings of the IEEE conference on computer vision and pattern recognition, 770–778.

Hemdan, E. E. D., Shouman, M. A., & Karar, M. E. (2020). COVIDX-Net: A framework of deep learning classifiers to diagnose COVID-19 in X-ray images. *arXiv preprint: 2003.11055*.

Huang, G., Liu, Z., Van Der Maaten, L., Weinberger, K. Q., et al. (2017). Densely connected convolutional networks. In *Proceedings of the IEEE Conference on Computer Vision and Pattern Recognition* (pp. 4700–4708).

Holshue, M. L., DeBolt, C., Lindquist, S., Lofy, K. H., Wiesman, J., Bruce, H., et al. (2020). First case of 2019 novel coronavirus in the United States. *The New England Journal of Medicine, 382*(10), 929–936.

Huang, C., Wang, Y., Li, X., Ren, L., Zhao, J., Hu, Y.i., et al. (2020). Clinical features of patients infected with 2019 novel coronavirus in Wuhan, China. *The Lancet, 395*(10223), 497–506.

ImageNet (2021). ImageNet: A Large-Scale Hierarchical Image Database. http://www.image-net.org/papers/imagenet_cvpr09.bi (Accessed January 17 2021).

Jain, R., Gupta, M., Taneja, S., & Hemanth, D. J. (2021). Deep learning based detection and analysis of COVID-19 on chest X-ray images. *Applied Intelligence, 51*(3), 1690–1700. https://doi.org/10.1007/s10489-020-01902-1

Kaggle (2020). https://www.kaggle.com/andrewmvd/convid19-X-rays (Accessed September 8 2020).

Kanne, J. P., Little, B. P., Chung, J. H., Elicker, B. M., & Ketai, L. H. (2020). Essentials for radiologists on COVID-19: An update—radiology scientific expert panel. *Radiology, 296*(2), E113–E114. https://doi.org/10.1148/radiol.2020200527

Khobahi, S., Agarwa, C., & Soltanalian, M., (2020). CoroNet: A deep network architecture for semi-supervised task-based identification of COVID-19 from chest X-ray images. medRxiv.

Kulkarni, S., Seneviratne, N., Baig, M. S., & Ahmed Khan, A. H. (2020). Artificial intelligence in medicine: Where are we now? *Academic Radiology, 27*(1), 62–70. https://doi.org/10.1016/j.acra.2019.10.001

Lee, Y. E., Ng, Y. M., & Khong, L. P. (2020). COVID-19 pneumonia: What has CT taught us? *The Lancet Infectious Diseases, 20*, 384–385. https://doi.org/10.1016/S1473-3099(20)30134

Li, H., Liu, S.-M., Yu, X.-H., Tang, S.-L., & Tang, C.-K. (2020). Coronavirus disease 2019 (COVID-19): Current status and future perspectives. *Journal of Antimicrobial Agents, 55*(5), 105951. https://doi.org/10.1016/j.ijantimicag.2020.105951

Luz, E., Silva, L. P., Silva, R., & Moreira, G. (2020). Towards an efficient deep learning model for covid-19 patterns detection in x-ray images. arXiv preprint:2004.05717.

Majeed, T., Rashid, R., Ali, D., & Asaad, A. (2020). Covid-19 detection using CNN transfer learning from x-ray images. medRxiv.

Minaee, S., Kafieh, R., Sonka, M., Yazdani, S., & Jamalipour Soufi, G. (2020). Deep-covid: Predicting covid-19 from chest x-ray images using deep transfer learning. *Medical Image Analysis, 65*, 101794. https://doi.org/10.1016/j.media.2020.101794

Narin, A., Kaya, C., & Pamuk, Z., (2020). Automatic Detection of Coronavirus Disease (COVID-19) Using X-Ray Images and Deep Convolutional Neural Networks. arXiv preprint:2003.10849.

Nayak, S. R., Nayak, D. R., Sinha, U., Arora, V., & Pachori, R. B. (2021). Application of deep learning techniques for detection of COVID-19 cases using chest X-ray images: A comprehensive study. *Biomedical Signal Processing and Control, 64*, 102365. https://doi.org/10.1016/j.bspc.2020.102365

Ohata, E. F., Bezerra, G. M., das Chagas, Neto, A. V. L., Albuquerque, A. B., et al. (2020). Automatic detection of COVID-19 infection using chest X-ray images through transfer learning. *IEEE/CAA Journal of Automatica Sinica, 8*(1), 239–248. https://doi.org/10.1109/JAS.2020.1003393

OpenCV (2021) Open Source Computer Vision (OpenCV) Library. https://github.com/opencv/opencv/wiki/CiteOpenCV (Accessed January 15 2021).

Ouchicha, C., Ammor, O., & Meknassi, M. (2020). CVDNet: A novel deep learning architecture for detection of coronavirus (Covid-19) from chest x-ray images. *Chaos, Solitons & Fractals, 140*, 110245. https://doi.org/10.1016/j.chaos.2020.110245

Ozturk, T., Talo, M., Yildirim, E. A., Baloglu, U. B., Yildirim, O., & Rajendra Acharya, U. (2020). Automated detection of COVID-19 cases using deep neural networks with X-ray images. *Computers in Biology and Medicine, 121*, 103792. https://doi.org/10.1016/j.compbiomed.2020.103792

Parah, S. A., Kaw, J. A., Bellavista, P., Loan, N. A., Bhat, G. M., Muhammad, K., et al. (2020). Efficient security and authentication for edge-based internet of medical things. *IEEE Internet of Things Journal*. https://doi.org/10.1109/JIOT.2020.3038009

Polat, Ç., Karaman, O., Karaman, C., Korkmaz, G., Balcı, M. C., & Kelek, S. E. (2021). COVID-19 diagnosis from chest X-ray images using transfer learning: Enhanced performance by debiasing dataloader. *Journal of X-Ray Science and Technology, 29*(1), 19–36. https://doi.org/10.3233/XST-200757

Rahimzadeh, M., & Attar, A., (2020). A New Modified Deep Convolutional Neural Network for Detecting COVID-19 from X-ray Images. arXiv preprint:2004.08052.

Rebouças Filho, P. P., Cortez, P. C., Barros, A. C.da. S., & de Albuquerque, V. H. C. (2014). Novel adaptive balloon active contour method based on internal force for image segmentation–a systematic evaluation on synthetic and real images. *Expert Systems with Applications, 41*(17), 7707–7721. https://doi.org/10.1016/j.eswa.2014.07.013

Rodrigues, M. B., Da Nobrega, R. V. M., Alves, S. S. A., Reboucas Filho, P. P., Duarte, J. B. F., Sangaiah, A. K., et al. (2018). Health of things algorithms for malignancy level classification of lung nodules. *IEEE Access, 6*, 18592–18601. https://doi.org/10.1109/Access.628763910.1109/ACCESS.2018.2817614

Sethy, K. P., Behera, K. S., Ratha, K. P., & Biswas, P. (2020). Detection of Coronavirus Disease (COVID-19) Based on Deep Features and Support Vector Machine. Preprints, 2020030300.

Shan, F., Gao, Y., Wang, J., Shi, W., Shi, N., Han, M., et al., (2020). Lung infection quantification of COVID-19 in CT images with deep learning, arXiv preprint: 2003.04655.

Simonyan, K., & Zisserman, A., (2014). Very deep convolutional networks for large-scale image recognition. arXiv, preprint:1409.1556.

Singh, A. K., Kumar, A., Mahmud, M., Kaiser, M. S., Kishore, A., et al. (2021). COVID-19 Infection detection from chest X-ray images using hybrid social group optimization and support vector classifier. *Cognitive Computation, 1–13*. https://doi.org/10.1007/s12559-021-09848-3

Vaid, S., Kalantar, R., & Bhandari, M. (2020). Deep learning COVID-19 detection bias: Accuracy through artificial intelligence. *International Orthopaedics, 44*(8), 1539–1542. https://doi.org/10.1007/s00264-020-04609-7

Wang, X., Peng, Y., Lu, L., Lu, Z., Bagheri, M., & Summers, R. M. (2017). Chestx-ray8: Hospital-scale chest x-ray database and benchmarks on weakly-supervised classification and localization of common thorax diseases. In *Proceedings of the IEEE conference on computer vision and pattern recognition* (pp. 2097–2106).

Wang, D., Hu, B., Hu, C., Zhu, F., Liu, X., Zhang, J., et al. (2020). Clinical characteristics of 138 hospitalized patients with 2019 novel coronavirus–infected pneumonia in Wuhan, China. *Journal of the American Medical Association, 323*(11), 1061. https://doi.org/10.1001/jama.2020.1585

Wang, L., & Wong, A. (2020). COVID-Net: A tailored deep convolutional neural network design for detection of COVID-19 cases from chest radiography images. *Scientific Reports, 10*, 19549. https://doi.org/10.1038/s41598-020-76550-z

Wang, S., Kang, B., Ma, J., Zeng, X., Xiao, M., Guo, J., et al. (2020). A deep learning algorithm using CT images to screen for Corona Virus Disease (COVID-19). *MedRxiv*. https://doi.org/10.1101/2020.02.14.20023028

Xie, X., Zhong, Z., Zhao, W., Zheng, C., Wang, W., & Liu, J. (2020). Chest CT for typical 2019-nCoV pneumonia: Relationship to negative RT-PCR testing. *Radiology, 296*, Article 200343. https://doi.org/10.1148/radiol.2020200343

Xu, X., Chen, P., Wang, J., Feng, J., Zhou, H., Li, X., et al. (2020). Evolution of the novel coronavirus from the ongoing Wuhan outbreak and modeling of its spike protein for risk of human transmission. *Science China Life Sciences, 63*(3), 457–460. https://doi.org/10.1007/s11427-020-1637-5

Zhang, J., Xie, Y., Li, Y., Shen, C., Xia, Y. (2020). COVID-19 screening on chest x-ray images using deep learning based anomaly detection. arXiv preprint: 2003.12338, 27.

Zhang, J., Xie, Y., Liao, Z., Pang, G., Verjans, J., Li, W., et al. (2020). Viral pneumonia screening on chest x-ray images using confidence-aware anomaly detection. arXiv preprint:2003.12338.